NOTES AND CORRESPONDENCE

Analysis of an Air Motion System on a Light Aircraft for Boundary Layer Research

R. WOOD, I. M. STROMBERG, P. R. JONAS, AND C. S. MILL

Department of Physics, University of Manchester Institute of Science and Technology, Manchester, United Kingdom

6 June 1996 and 20 November 1996

ABSTRACT

A system has been developed for use on a light aircraft for the measurement of the turbulent wind vector components that does not rely on the use of either an inertial navigation system (INS) or Doppler radar. The system described here uses a five-hole probe to measure the wind vector relative to the aircraft. A GPS system, a vertical gyroscope for aircraft pitch and roll angles, a gyrocompass system, and a strap-down three-axis accelerometer system are used to obtain aircraft motion. Flight tests and results of an intercomparison with the United Kingdom Meteorological Office C-130 are presented. Under conditions of straight and level flight, the estimated rms errors are 0.3 m s^{-1} for the vertical wind component and 2 m s^{-1} for the horizontal components.

1. Introduction

Measurements of air velocity using instrumented aircraft are of prime importance to meteorological studies, and a high degree of accuracy is required to ascertain atmospheric parameters such as turbulent fluxes. Several authors have described measurement techniques for the measurement of wind velocity using aircraft (Axford 1968; Lenschow 1986; Tjernstrom and Friehe 1991; Crawford and Dobosy 1992) and so a detailed account of the methods is not presented here. Essentially, it is necessary to measure both the air velocity relative to the aircraft and the velocity of the aircraft relative to the ground to a high degree of accuracy to obtain accurate wind measurements. In this paper, a wind measurement system is described for use on a light aircraft that does not require an inertial navigation system (INS) to measure the aircraft velocity but instead uses a combination of accelerometers, static pressure altitude, and global positioning system (GPS). The wind vector relative to the aircraft is obtained using pressure measurements on a boom (Brown et al. 1983). In-flight and ground-based instrument calibrations are discussed, and results of flight tests and an intercomparison with the U.K. Meteorological Office C-130 are presented.

Corresponding author address: Mr. Robert Wood, Department of Physics, University of Manchester Institute of Science and Technology, P.O. Box 88, Manchester M60 1QD, United Kingdom. E-mail: bobby@cloudz.phy.umist.ac.uk

2. Air motion and other related instrumentation on the UMIST Cessna 182

a. Background

A single-engine Cessna 182 aircraft (Fig. 1) has been modified to house equipment inside the cabin and operate various probes located both on the wings and inside the aircraft. Since 1986 research flights have included marine aerosol studies (Smith et al. 1989) and atmospheric trace gas measurements (Choularton et al. 1995; Gallagher et al. 1990, 1991, 1994), together with studies of the radiative properties of clouds. Since 1992 the emphasis has increasingly moved toward work requiring air motion measurements. The aim of the work reported here has been to design and test a system for air motion measurement that is optimized for use on a light aircraft. A summary of the instrumentation on the Cessna-182 is given in Table 1.

b. Instrumentation

A five-hole probe is used to measure accurately the wind vector relative to the aircraft. This is an in-house design consisting of a pressure sensing head similar to the Rosemount type AJ 858 probe and is shown in Fig. 1. The probe tip is hemispherical and has a 30-mm diameter with five pressure ports to measure pitot-static differential pressure and the attack and sideslip differential pressure. The measured pressures, together with air temperature, are used to calculate true airspeed and angles of attack and sideslip. The instantaneous wind vector components relative to the aircraft can then be calculated. The five-hole probe head is located 960 mm

FIG. 1. The Cessna 182 aircraft showing the position of the five-hole probe.

TABLE 1. Summary of parameters measured, with sampling rate, resolution, and range.

Name	Instrument	Sampling rate (Hz)	Resolution	Range
Five-hole probe				
Pitot-static pressure	Eurosensor	20.0	0.03 hPa	0–67 hPa
Static pressure	Eurosensor	20.0	0.5 hPa	600–1150 hPa
Differential pressure (attack)	Eurosensor	20.0	0.03 hPa	±60 hPa
Differential pressure (sideslip)	Eurosensor	20.0	0.03 hPa	±60 hPa
Accelerometer system				
Vertical acceleration	Eurosensor 3026-005-P	20.0	0.01 m s^{-2}	±2*g*
Lateral acceleration	Eurosensor 3026-005-P	20.0	0.01 m s^{-2}	±2*g*
Longitudinal acceleration	Eurosensor 3036-005-P	20.0	0.01 m s^{-2}	±2*g*
Gyroscope–compass system				
True heading	King KCS55A	20.0	0.087°	0°–360°
Pitch angle	King KVG 350	20.0	0.006°	±12.5°
Roll angle	King KVG 350	20.0	0.006°	±12.5°
GPS navigation system	Garmin GPS 100			
Latitude		1.0	0.00017°	±90°
Longitude		1.0	0.00017°	±180°
Ground speed		1.0	0.05 m s^{-1}	0–300 m s^{-1}
Track across ground		1.0	0.1°	0°–360°
Altitude		1.0	0.5 m	0°–10 000 m
Atmospheric state data				
Temperature (total)	PT100 Rosemount	1.0	0.02°C	−50°–50°C
Temperature (reverse flow)	UMIST	1.0	0.02°C	−50°–50°C
Dewpoint	Michell hygrometer	1.0	0.03°C	−30°–50°C
Other measurements				
Radiation	2 Eppley PSP (285–2800 nm)	1.0	0.25 W m^{-2}	0–1000 W m^{-2}
Radar altitude	King	1.0	0.5 m	0–800 m

ahead of the starboard wing immediately outboard of the wing strut and 2.4 m inboard from the wing tip (Fig. 1). The probe electronics, together with a three-axis accelerometer system described later, are housed in a pod that also supports the probe boom. The pod is a standard unit manufactured by Particle Measuring Systems, Inc. for the FSSP 100. The system is self-contained, requiring only power to produce a 12-bit digitized data output.

The static pressure port is installed coaxially on the probe boom 280 mm to the rear of the pressure-sensing head and consists of a ring of 10 1.2-mm-diameter holes that connect to an internal annular groove sealed by O-rings. The inner cavity connects through the tube wall to the absolute static pressure transducer. This design of static pressure port is less affected by changes in attack and sideslip angles than conventional flat-plate pressure ports.

Air temperature is measured using a Rosemount total temperature probe type 102 mounted under the aircraft wing. A recovery factor of 0.91 has been calculated from flight tests and is used to derive the static air temperature (Hacker and Schwerdtfeger 1988). Navigation data are obtained using a Garmin GPS 100 system with a typical accuracy of 100 m. In case of poor GPS coverage a Litton Omega system is used as a backup.

The Cessna is fitted with a King KVG 350 vertical gyroscope to measure the aircraft attitude angles of pitch and roll at 20 Hz. Tests indicate that the random error in these measurements is less than 0.02°, with a systematic offset of less than 0.25°. The systematic error introduces a maximum possible offset in the mean vertical wind of around 0.25 m s^{-1}. The gyroscope is mounted in the main body of the aircraft close to the aircraft's center of gravity.

Aircraft heading is measured using a King KCS55A slaved gyrocompass system accurate to better than 1°. Three orthogonal piezoresistive Eurosensor type 3026-005-P accelerometers located in the five-hole probe pod are used to determine the three velocity components of the probe. The distance between the accelerometers and the pressure-sensing head of the five-hole probe is less than 1.5 m. The accelerometer system is housed in a temperature-controlled oven within the five-hole probe pod, 1.2 m aft of the probe head. The range of the accelerometers is ± 5 *g*, at up to 350 Hz, and their resonant frequency is 600 Hz. The accelerometers are mounted so that they record accelerations along the longitudinal, lateral, and local vertical axes of the five-hole probe. Corrections are made to take into account the motion of the probe head relative to the accelerometers using rates of change of the attitude angles derived from the gyroscopes and compass.

3. Calibration of attack and sideslip angles

The airflow vector is defined by its magnitude (the true airspeed) and the angles of attack and sideslip whose coordinate system is fixed relative to the aircraft (Axford 1968). These parameters require in-flight calibration since airflow around the probe and around the aircraft itself cannot be determined from ground-based calibration.

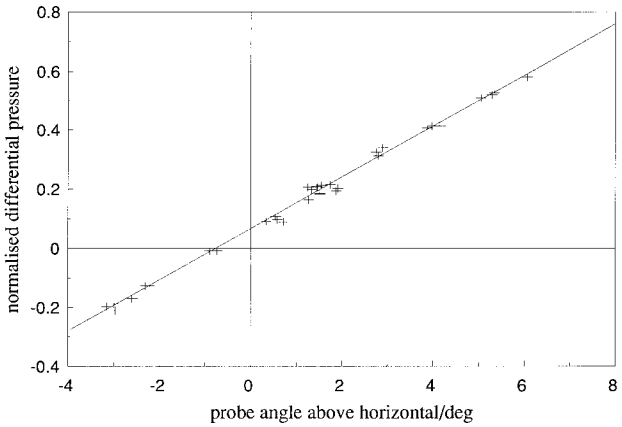

FIG. 2. Results of the 27 attack-angle calibration runs. For each run the mean differential pressure across the attack angle ports normalized with the mean pitot-static differential pressure is calculated and plotted against the mean probe angle relative to the earth horizontal. The results indicate that $K_\alpha = 0.086 \pm 0.005$ and $\alpha_o = 0.71 \pm 0.19$.

For the vertical component of air motion, the attack angle is of prime significance and must be known accurately. The attack angle α is related to the differential pressure ΔP_α across the two attack ports (Brown et al. 1983) by

$$\alpha = K_\alpha^{-1} \Delta P_\alpha (P_t - P_s)^{-1} - \alpha_o, \qquad (1)$$

where K_α is the attack-angle sensitivity factor determined by in-flight calibration detailed below and $P_t - P_s$ is the pitot-static differential pressure. The attack-angle offset α_o is included to take into account the distortion of the airflow vector by the aircraft–probe.

By physically varying the angle that the probe makes with the aircraft's longitudinal axis and carrying out straight and level runs, the effect of the airflow distortion around the aircraft wing can be investigated. This was carried out by modification of the probe mounting so that nine different attitudes were available. A total of 34 straight and level runs of 25 km were flown in still air over the sea at 1100 m. The results are shown in Fig. 2. Mean values of $\Delta P_\alpha (P_t - P_s)^{-1}$ are plotted as a function of the mean angle of the probe above the horizontal for each run. Linearity of the graph over a range of almost 10° can be seen (regression coefficient of 0.9989). From these flights, along with a ground-based pressure calibration, a value of $K_\alpha = 0.086 \pm 0.005$ and an offset angle of $\alpha_o = 0.71°$ were found. The K_α value is close to the theoretical prediction of $K_\alpha = 0.078$ (Brown et al. 1983). The attack-angle offset is caused by deflection of the airflow ahead of the wing beneath which the probe is mounted. From analysis of the flight and ground-based calibration data the attack-angle mea-

surement accuracy is better than 0.25°. The sideslip angle β is a function of the differential pressure across the sideslip ports using a similar relation to that for the attack angle.

For an isolated axisymmetric probe moving through an airstream, the attack and sideslip angle sensitivity factors would be identical. From yawing oscillation tests described by Bogel and Baumann (1991), a 4% difference in the sensitivity factors was discovered for a Rosemount type 858 flow angle sensor mounted on a boom extending from the nose of the DLR Falcon aircraft. At present we assume that the attack and sideslip sensitivity factors are identical, but we plan to investigate this further.

The sideslip offset β_o has been determined using reciprocal wind calibration runs, also known as K, γ runs (Offiler et al. 1994). Providing the conditions of smooth air, homogeneity, and constant horizontal wind speed are met, these runs can be used to isolate the sideslip offset. The tests indicate a value of $\beta_o = 4.7 \pm 0.9°$.

4. Computation of vertical air motion

A single instrument cannot provide the vertical component of aircraft velocity, and so a combination of two sensors is used: the static pressure signal is accurate in the long term but noisy over short timescales; the vertical accelerometer is accurate over short timescales but tends to drift in the long term.

Several methods for the use of the high-frequency accuracy of the accelerometers and the low-frequency accuracy of the static pressure transducer have been tested on aircraft. Shao et al. (1990) describe a method that uses Fourier filtering techniques. Blanchard (1971) and Lenschow (1986) describe another method by which the accuracy of the vertical aircraft motion can be increased significantly using a barometric feedback loop. The system we have adopted is to use a third-order barometric feedback loop similar to that described by Lenschow (1986). The feedback constants are determined by allowing the feedback system to have three real roots and a time constant set according to the relative accuracies, response times, and drifts of the accelerometer and the static pressure signals. Taking into account accelerometer and static pressure errors, the rms error in the vertical component of the aircraft velocity is less than 0.2 m s^{-1}.

5. Flight tests to determine vertical wind accuracy

a. Flight maneuvers

Flight maneuvers are essential in the evaluation of an airborne wind-measuring platform. From flight maneuvers documented by Axford (1968), Nicholls (1980), and Lenschow (1986), errors in many of the crucial parameters required to determine wind components can be identified and corrected. These include constant offset errors and response time (phase) errors that are difficult, if not impossible, to evaluate using ground-based tests. We have performed flight maneuvers using the UMIST aircraft as documented below. From the results, modifications both to software and hardware have been made, with the final conclusion being that the rms error in the vertical wind is less than 0.3 m s^{-1}.

Pitching oscillation tests (Lenschow 1986) were carried out by the pilot inducing a sinusoidal pitching oscillation with an amplitude of 4°–8°. We performed the tests at two frequencies: low frequency oscillations at 0.03–0.05 s^{-1} and high frequency oscillations at 0.5–1 s^{-1}. The modulation of the pitch angle modulates the true airspeed V_a, the aircraft vertical velocity w_p, and to a smaller extent the attack angle α; any modulation in derived vertical wind is assumed to arise from the maneuver itself rather than from atmospheric motion, provided the test is carried out in smooth air. Figure 3 displays time series from a low-frequency test (Fig. 3a) and a high-frequency test (Fig. 3b). The rms of the vertical wind component w is in both cases over one order of magnitude less than the rms of w_p, demonstrating that to a great extent the effects of the aircraft velocity are accounted for. The mean of the rms values of w from four tests is 0.412 m s^{-1}, while the corresponding value for w_p is 4.46 m s^{-1}. Four straight and level runs in the same air gave a background rms value of 0.326 m s^{-1} for w, with a mean rms of 0.360 m s^{-1} for w_p. This suggests that much of the variation in w during the pitching maneuvers is due to atmospheric motion rather than errors in the wind-measuring system, although background noise in the measurement system could account for some of this variation.

b. Intercomparison flight with Meteorological Office C-130

During the Terrestrial Initiative on Global Environmental Research (TIGER) project, the Meteoreological Office C-130 was available to make intercomparison runs in order to further test the validity of the Cessna 182 wind-measuring system. Because of the difference in normal operating speeds between the two aircraft, a side-by-side intercomparison between the two, as documented in Nicholls et al. (1983) and Lenschow et al. (1991), was impossible. Instead, runs of fixed track and altitude were flown, with the Cessna starting the runs at an earlier time than the C-130 so as to end the runs with the aircraft as close together as possible. GPS was used for horizontal position and to compute the distance of the aircraft along the fixed track. This allowed us to compare spatial series of vertical wind and temperature. The lateral separation of the aircraft tracks was less than 350 m at all times on the runs, and the runs were flown in a well-mixed boundary layer with strong surface heating.

Spatial series of w from two runs are shown in Fig. 4, and their respective power spectra are shown in Fig.

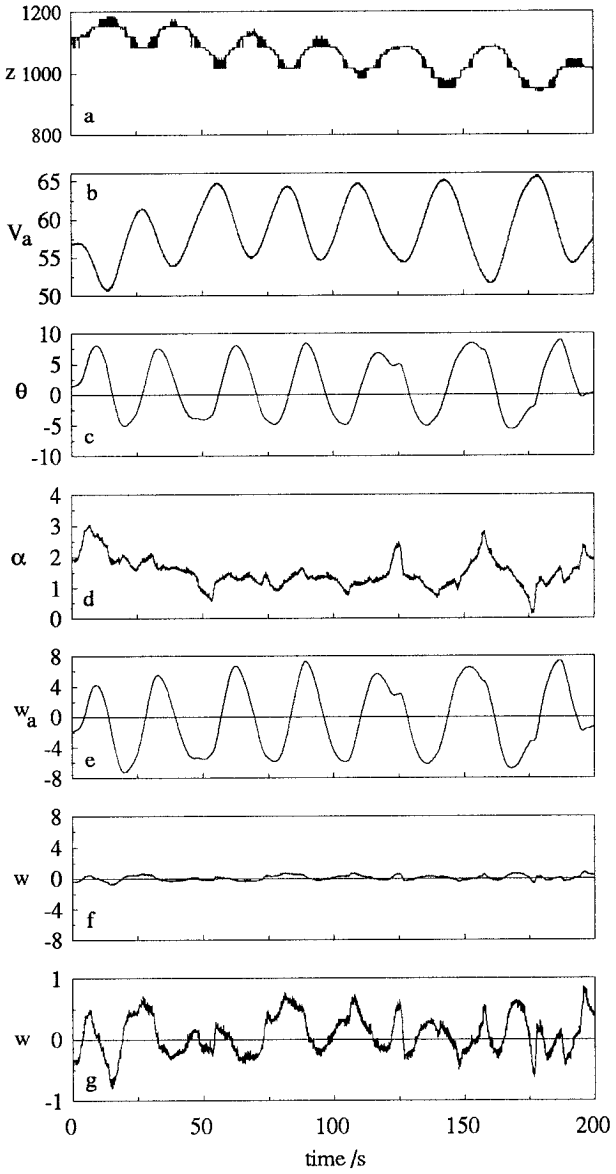

FIG. 3a. Results of a low-frequency pitch oscillation test used to elucidate errors in the amplitudes and phases of the key parameters necessary for the computation of the vertical wind component. Shown are 200-s time series of (a) altitude z, (b) true airspeed V_a, (c) pitch angle θ, (d) attack angle α, and (e) vertical aircraft velocity w_p. The derived vertical wind component w is shown in (f) using the same scale as that for the vertical aircraft velocity and in (g) using a magnified scale. The units are meters for altitude, meters per second for velocities, and degrees for angles.

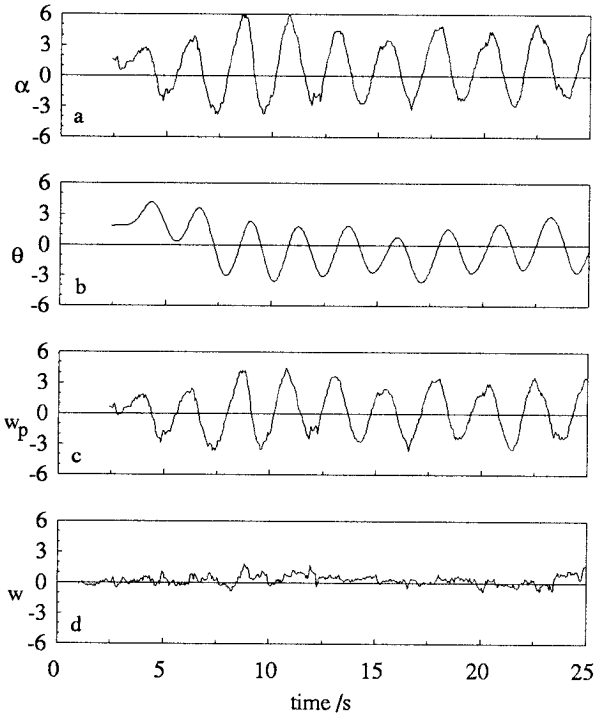

FIG. 3b. Time series of important parameters from a high-frequency pitch oscillation test. Shown are 25-s time series of (a) attack angle α, (b) pitch angle θ, (c) vertical aircraft velocity w_p, and (d) vertical wind component w. The units are meters per second for velocities and degrees for angles.

5a. Run a was at 150 m above sea level, run b at 650 m. The spatial series show that many of the larger features are common to both the C-130 and the Cessna data, although there are inevitable differences due to the time difference in the sampling between the two aircraft on any run. Figure 5b shows the ratio of the C-130/Cessna power spectra for each of the runs. The power spectra show good agreement for wavenumbers up to around 0.02 m^{-1}. Deviations at higher wavenumbers are seen because both C-130 power spectra exhibit unexpected peaks at wavenumbers in the range 0.09–0.14 m^{-1} (Fig. 5a), corresponding to frequencies between 9 and 14 Hz, respectively. The peaks are not present in the Cessna power spectra and may arise from resonances of the noseboom on the C-130, on the end of which are mounted the vanes for measurement of attack and sideslip angles.

Means and standard deviations of vertical wind and temperature measured by the Cessna and the C-130 are presented in Table 2. It is more than likely that the nonzero mean vertical velocities are attributable to undetermined offsets in the attack and/or pitch angles. The rms vertical velocities compare very well for both runs. The temperature measurements are corrected for dynamic heating effects using the true airspeed. The differences in the mean temperature measured by the two aircraft are 0.14° and 0.27°C for runs 1 and 2, respectively, with the C-130 recording the higher temperature on both runs. The rms temperature variations compare to within 6% on run 2 but differ more on run 1. The reason for this discrepancy is not known, although similar differences were found in a side-by-side comparison between the U.K. Meteorological Office C-130, the DLR Falcon, and the CAM Merlin (Quante et al. 1996).

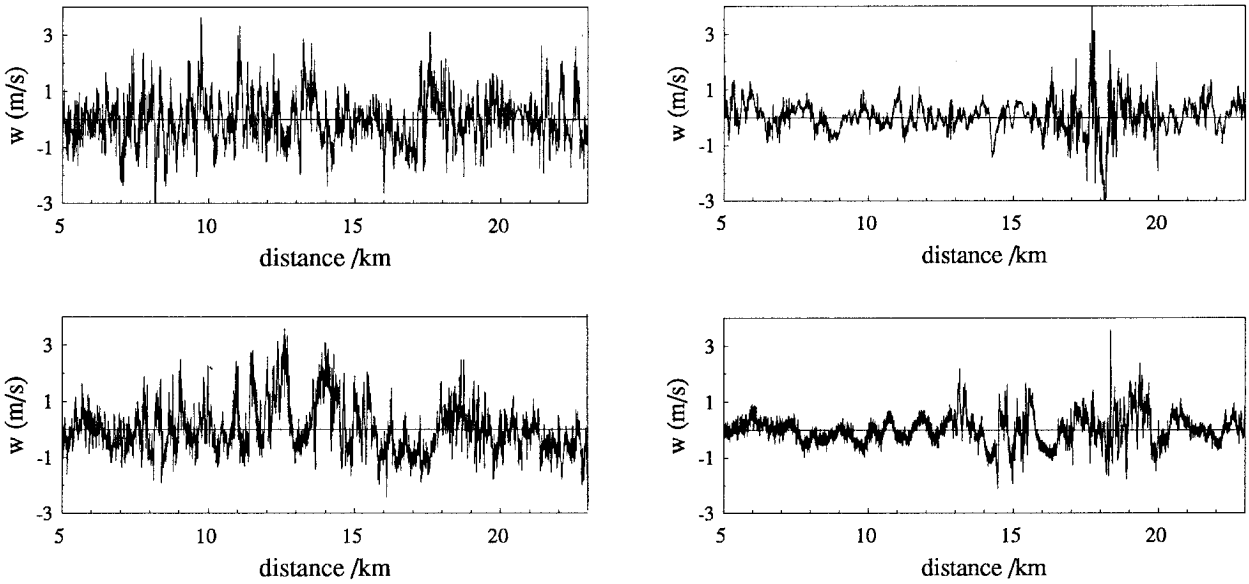

FIG. 4. Spatial series of the vertical wind component for two runs as measured by the Cessna (top) and C-130 (bottom) during the intercomparison flight of 3 June 1993. Run 1 (left) is at an altitude of 200 m, run 2 (right) at 600 m.

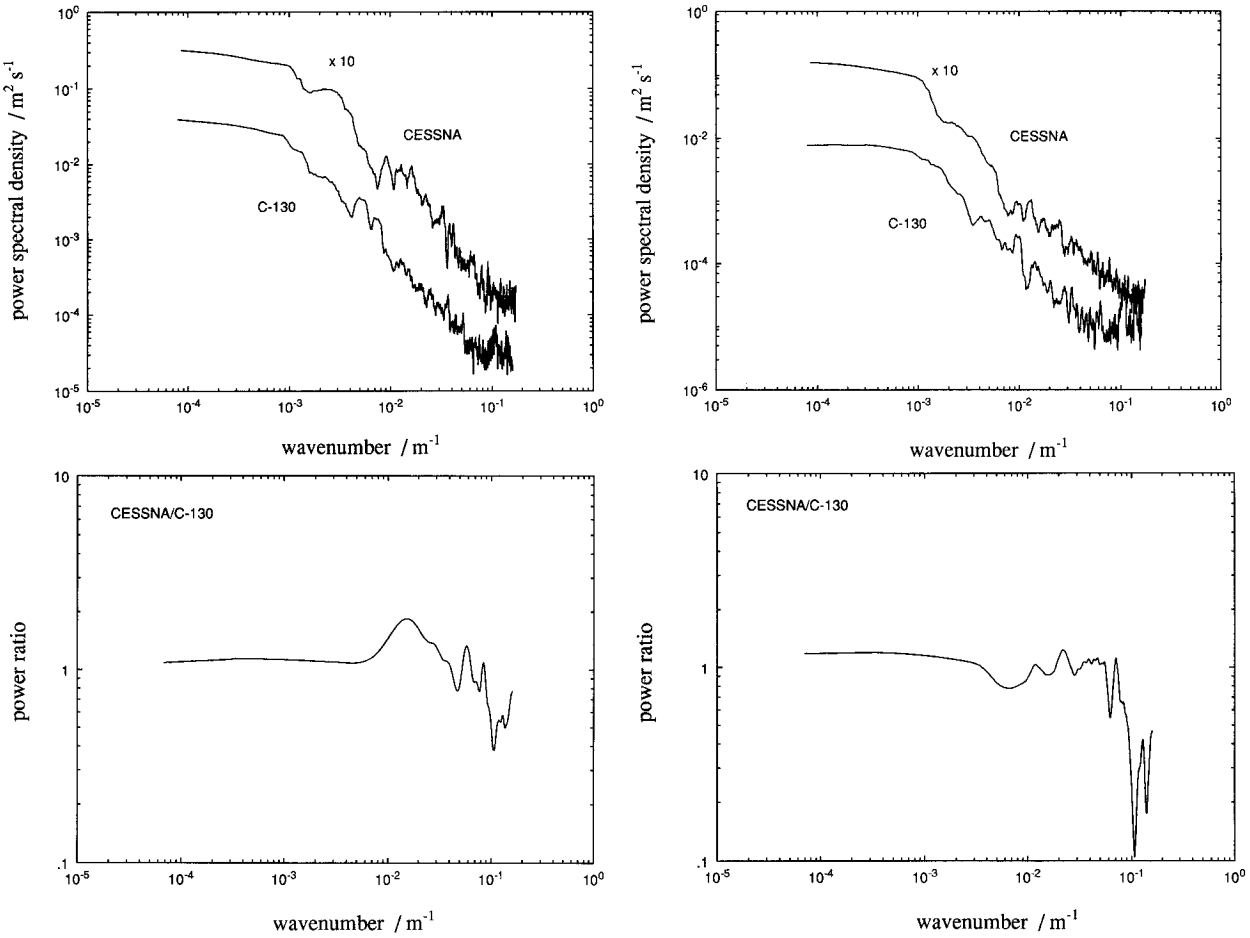

FIG. 5. Power spectra (a) and ratio of spectra (b) of vertical wind for the intercomparison runs 1 (left) and 2 (right) for the Cessna and the C-130, plotted as a function of wavenumber. The Cessna data are multiplied by a factor of 10 (top spectra only) to aid visualization.

TABLE 2. Mean and rms vertical wind components and temperatures measured by the Cessna and the C-130 from the two intercomparison runs discussed in the text. The units of quantities involving velocity are meters per second and temperatures are measured in degrees Celsius.

	Run 1		Run 2	
	Cessna	C-130	Cessna	C-130
$\bar{w}$	0.122	−0.171	−0.020	−0.309
σ_w	0.837	0.848	0.568	0.530
$\bar{T}$	10.83	10.97	8.76	9.03
σ_T	0.245	0.511	0.535	0.506

It is hoped that further, more extensive intercomparisons can be made between the two aircraft.

c. Reciprocal runs

A further test of the accuracy of the vertical wind component is the reciprocal runs test. The rms value of the vertical wind for both forward and reciprocal legs should be equal if the measurements are accurate. A total of 13 such runs of between 12 and 24 km were carried out on five flights. The values of σ_w measured on each leg are plotted against each other (Fig. 6). The results indicate that, assuming the conditions were homogeneous, the difference in σ_w calculated for the two runs is typically 0.1 m s^{-1} or less. While the reciprocal runs indicate that the measurements of vertical wind using the Cessna are consistent, it is not possible to infer information on the absolute accuracy of the system using this technique.

6. Computation of horizontal wind components

a. Calculation of aircraft horizontal velocity

Computation of horizontal winds requires precise knowledge of the components of the aircraft's horizontal velocity over the ground. Integrated acceleration, as in the computation of the vertical component of aircraft velocity, accurately provides these in the short term, and several methods have been employed by researchers to correct the data for the accelerometer drift. Shaw (1988) uses Loran C navigational data, while Leach and MacPherson (1991) apply Kalman filtering techniques and both Doppler and Litton data to correct for horizontal accelerometer drift. We use the accuracy of GPS as a long-term navigational reference for our system. The GPS signal is logged at 1 Hz and has an accuracy in the horizontal generally better than 100 m. Currently, horizontal winds are computed using Fourier filtering methods, but phase errors due to this technique require that a more advanced method be employed. We plan to use symmetric filters to detect and remove phase errors in the matching of accelerometer and GPS data in the near future.

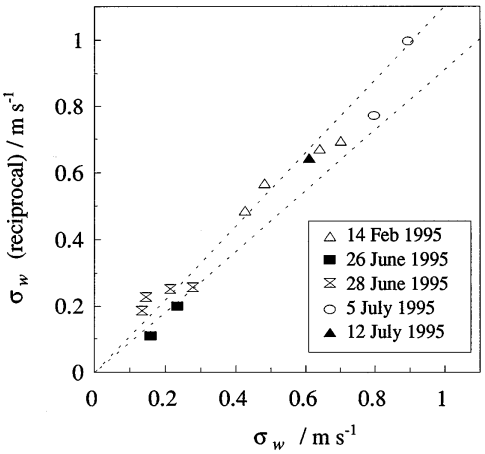

FIG. 6. Root-mean-square vertical wind results for 13 reciprocal wind calibration runs. The rms value of vertical wind measured on the reciprocal leg is plotted against the corresponding value measured on the forward leg. The dotted lines indicate 10% error.

b. Computation of the horizontal wind components

The horizontal components of the airflow relative to the five-hole probe in the aircraft coordinate system are transformed into an earth-based fixed coordinate system with eastward and northward axes using the aircraft heading obtained from the gyrocompass. Initially the compass data on the aircraft were fed only into the Litton Omega navigation system and as such is updated only once every few seconds with an undetermined time delay. We have now digitized the compass synchro signal directly and it is sampled by the main data acquisition system at 20 Hz. The tests detailed below, however, used the old system for heading data.

c. Flight tests to assess the accuracy of the horizontal wind components

In order to test the accuracy of the horizontal wind measurements, reciprocal wind calibration (RWC) runs detailed in section 3 have been flown (Lenschow 1986; Offiler et al. 1994). Figure 7 shows the results of 13 RWC runs. Runs were defined and executed using real-time GPS navigational data to maintain constant track over ground on both legs. Figure 7a is a comparison of the mean along-track wind calculated for each leg of the run, while Fig. 7b is a comparison of the mean cross-track wind calculated for the same runs. The dotted lines indicate an error of 10%. Reasonable agreement is found in both the along-track and cross-track mean winds measured on each leg, although there appears to be a bias in the cross-track winds; the measured cross-track wind component is greater on the leg where the wind is from the starboard side. This bias could be the result of flow distortion around the aircraft wing that is dependent on the sideslip angle. We hope that further flight trials, including the yawing maneuver suggested by Bogel and

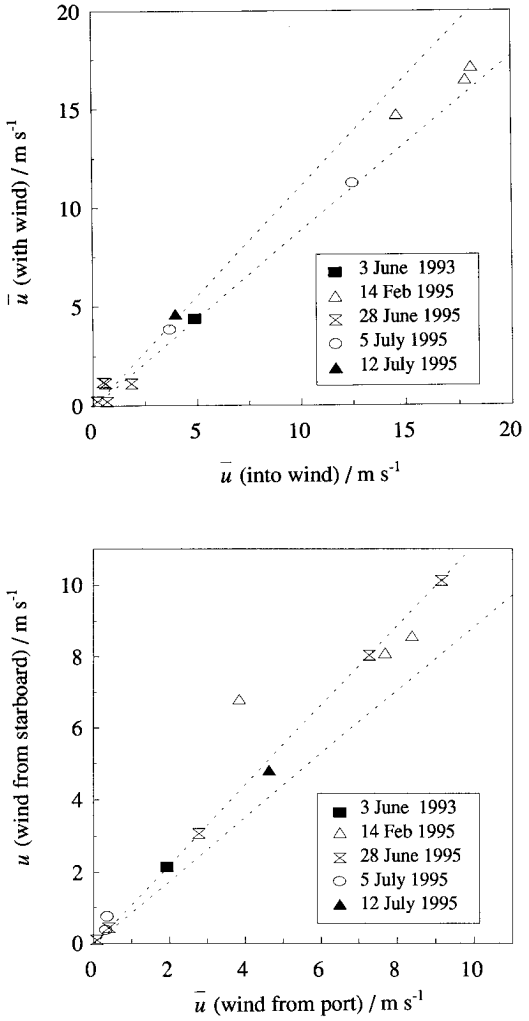

FIG. 7. Mean along-track (a) and cross-track (b) wind measurements from reciprocal wind calibration runs. The value of the wind component measured on the two legs are plotted against each other. The dotted lines indicate 10% error.

Baumann (1991), will be useful in isolating this source of error.

Horizontal velocity components were measured for the intercomparison runs with the Meteorological Office C-130, as detailed above. The results shown in Table 3 indicate that the mean horizontal wind components measured using our system are comparable with those measured using the C-130. The cross-track bias mentioned above is borne out by these data; the magnitude of $\bar{u}$ (the cross-track component, since the runs were southward and northward, respectively) measured by the Cessna is less than that measured by the C-130 on run 1, where the wind is from the port side, and greater for run 2, where the wind is from the starboard side. The values of $\bar{v}$ measured by the two aircraft agree to better than 10%. Similar agreement is seen in the values of σ_v. The discrepancy in the σ_u values is more than likely to result from the aforementioned heading angle synchronization problem.

TABLE 3. Mean and rms horizontal wind components measured by the Cessna and the C-130 from the two intercomparison runs discussed in the text. The units of all quantities are meters per second.

	Run 1		Run 2	
	Cessna	C-130	Cessna	C-130
$\bar{u}$	−3.991	−4.496	−2.327	−1.655
σ_u	1.145	1.364	1.795	0.852
$\bar{v}$	5.906	6.547	2.652	2.806
σ_v	0.991	0.884	1.163	1.138

7. Conclusions

The wind measuring system described here was developed as a low-cost alternative to the more expensive INS systems. We have used an in-house probe design mounted under the starboard wing of the aircraft. On the probe are mounted the pressure sensors necessary for the measurement of the velocity of the air relative to the five-hole probe. Within the probe housing three orthogonal temperature-controlled strapdown accelerometers are used to compute the vertical motion of the probe. To compensate for errors in the aircraft velocity arising from accelerometer drift, the acceleration data are combined with long-term reference data: static pressure for the vertical component and GPS for the horizontal components.

In the pitch oscillation tests, the rms vertical wind was at least 10 times smaller than the rms aircraft vertical component of velocity, indicating that the effect of aircraft vertical motion has been largely accounted for. A comparison flight with the Meteorological Office C-130 aircraft gave excellent agreement of the rms values of the vertical wind and the mean temperatures. A comparison of the power spectra revealed broad agreement, except at high frequency where the C-130 power spectra generally contained more energy, with broad peaks at frequencies between 9 and 14 Hz. In addition, reciprocal runs to investigate the consistency of the system gave good agreement in the rms vertical wind measured on the forward and reciprocal legs. Results from all the tests for the accuracy of the vertical wind indicate the errors in this measurement are of the order of 10%.

Reciprocal wind calibration runs and the intercomparison flight with the Meteorological Office C-130 demonstrate reasonable accuracy in the mean horizontal wind components. High-frequency information is not yet trustworthy due to the slow logging rate and synchronization problems of the heading signal, but with the planned changes it should be obtainable in the near future.

Acknowledgments. We are grateful to Alan Lee and Peter Kelly for their continued technological help in the construction and modification of the sensors on the air-

craft. We thank the United Kingdom Natural Environment Research Council for supporting this work, British Aerospace (Woodford) for their generous provision of equipment and hangarage, and the U.K. Meteorological Office for the provision of the C-130 aircraft.

REFERENCES

Axford, D. N., 1968: On the accuracy of wind measurements using an inertial platform in an aircraft and an example of a measurement of the vertical mesoscale of the atmosphere. *J. Appl. Meteor.*, **7,** 645–666.

Blanchard, R. L., 1971: A new algorithm for computing inertial altitude and vertical velocity. *IEEE Trans. Aerosp. Electron. Syst.*, **AES 7,** 1143–1146.

Bogel, W., and R. Baumann, 1991: Test and calibration of the DLR Falcon wind measuring system by maneuvers. *J. Atmos. Oceanic Technol.,* **8,** 5–18.

Brown, E. N., C. A. Friehe, and D. H. Lenschow, 1983: The use of pressure fluctuations on the nose of an aircraft for measuring air motion. *J. Climate Appl. Meteor.,* **22,** 171–180.

Choularton, T. W., M. W. Gallagher, K. N. Bower, D. Fowler, M. Zahniser, and A. Kaye, 1995: Trace gas flux measurements at the landscape scale using boundary-layer budgets. *Philos. Trans. Roy. Soc. London, Ser. A,* **351,** 357–369.

Crawford, T. L., and R. J. Dobosy, 1992: A sensitive fast-response probe to measure turbulence and heat flux from any airplane. *Bound.-Layer Meteor.,* **59,** 257–278.

Gallagher, M. W., and Coauthors, 1990: Case studies of the oxidation of sulphur dioxide in a hill cap cloud using ground and aircraft based measurements. *J. Geophys. Res.,* **95** (D11), 18 517–18 537.

——, and Coauthors, 1991: Measurements of the entrainment of hydrogen peroxide into cloud systems. *Atmos. Environ.,* **25A** (9), 2029–2038.

——, T. W. Choularton, K. N. Bower, I. M. Stromberg, and K. M. Beswick, 1994: Measurements of methane fluxes on the landscape scale from a wetland area in north Scotland. *Atmos. Environ.,* **28** (15), 2421–2430.

Hacker, J. M., and P. Schwerdtfeger, 1988: The FIAMS Research Aircraft System description. FIAMS Tech. Rep. 8, 70 pp. [Available from Flinders Institute for Atmospheric and Marine Sciences, Flinders University of South Australia, Bedford Park 5042, Australia.]

Leach, B. W., and J. I. MacPherson, 1991: An application of Kalman filtering to airborne wind measurement. *J. Atmos. Oceanic Technol.,* **8,** 51–65.

Lenschow, D. H., 1986: Aircraft measurements in the boundary layer. *Probing the Atmospheric Boundary Layer,* D. H. Lenschow, Ed., Amer. Meteor. Soc., 39–55.

——, E. R. Miller, and R. B. Friesen, 1991: A three-aircraft intercomparison of two types of air motion system. *J. Atmos. Oceanic Technol.,* **8,** 41–50.

Nicholls, S., 1980: The measurement of flight level wind and aircraft position by the MRF Hercules. MRF Internal Note 9, 67 pp. [Available from Meteorological Research Flight, Building Y46, DRA, Farnborough, Hampshire, GU14 6TD, United Kingdom.]

——, W. Shaw, and T. Hauf, 1983: An intercomparison of aircraft turbulence measurements made during JASON. *J. Climate Appl. Meteor.,* **22,** 1637–1648.

Offiler, D., P. R. A. Brown, A. L. M. Grant, W. D. N. Jackson, and D. W. Johnson, 1994: Report of the Aircraft Winds Working Group. MRF Tech. Note 17, 148 pp. [Available from Meteorological Research Flight, Farnborough, Hampshire, GU14 6TD, United Kingdom.]

Quante, M., P. R. A. Brown, R. Baumann, B. Guillemet, and P. Hignett 1996: Three-aircraft intercomparison of dynamical and thermodynamical measurements during the pre-EUCREX campaign. *Bietr. Phys. Atmos.*, **69,** 129–146.

Shao, Y., J. M. Hacker, and R. A. D. Byron-Scott, 1990: Airborne measurements in a coastal atmospheric boundary layer. FIAMS Research Rep. 48, 81 pp. [Available from Flinders Institute for Atmospheric and Marine Sciences, Flinders University of South Australia, Bedford Park 5042, Australia.]

Shaw, W. J., 1988: Inertial drift correction for aircraft-derived wind fields. *J. Atmos. Oceanic Technol.,* **5,** 774–782.

Smith, M. H., I. E. Consterdine, and P. M. Park, 1989: Atmospheric loadings of maritime aerosol during a Hebridean Cyclone. *Quart. J. Roy. Meteor. Soc.*, **115,** 383–395.

Tjernström, M., and C. A. Friehe, 1991: Analysis of a radome airmotion system on a twin-jet aircraft for boundary layer research. *J. Atmos. Oceanic Technol.,* **8,** 19–40.